Proton Slip of the Chloroplast ATPase: Its Nucleotide Dependence, Energetic Threshold, and Relation to an Alternating Site Mechanism of Catalysis[†,‡]

Georg Groth and Wolfgang Junge*

Biophysik, Fachbereich Biologie/Chemie, Universität Osnabrück, D-49069 Osnabrück, Germany

Received March 15, 1993; Revised Manuscript Received May 18, 1993

ABSTRACT: The F-ATPase of chloroplasts couples proton flow to ATP synthesis, but is leaky to protons in the absence of nucleotides. This "proton slip" can be blocked by small concentrations of ADP or by inhibitors of the channel portion, CF_0. We studied charge flow through the ATPase by flash spectrophotometry and analyzed the inhibition of proton slip by nucleotides, phosphate/arsenate, and insufficient proton motive force. The following inhibition constants (at given background concentrations) were observed: ADP, 0.2 μM (0.5 mM P_i); ADP, 13.4 μM (no P_i); P_i, 43 μM (1 μM ADP); GDP, 2.5 μM (0.5 mM P_i); ATP, 2 μM. ADP and P_i mutually lowered their respective inhibition constants. Phosphate could be replaced by arsenate. Proton slip occurred only if the proton motive force exceeded a certain threshold, similar to that for ATP synthesis. The inhibition of proton slip by ADP and GDP qualified the respective nucleotide binding sites as belonging to the subset of two (or three) potentially catalytic sites out of the total of six. We interpreted the ADP-induced transition between different conduction states of the ATPase from "slipping" to "closed" to "coupled" as a consequence of the alternating site mechanism of catalysis. Whereas the proton translocator idles in the absence of nucleotides, the high-affinity binding of the first ADP/P_i couple to one site clutches proton flow to some (conformational) change that can only be executed after the binding of another ADP/P_i couple to a second site. From there on these sites alternate in the catalytic cycle. An entropic machine is presented which likewise models proton slip, unisite, and multisite ATP synthesis and hydrolysis.

Driven by proton motive force across the thylakoid membrane, the F-ATPase of chloroplasts, CF_0CF_1,[1] can conduct protons in two different ways: (a) proton translocation coupled to ATP synthesis and (b) uncoupled proton transport ("proton slip") in the absence of nucleotides. If the channel portion, CF_0, is exposed by removal of the catalytic portion, CF_1, it acts as a highly specific proton channel. These CF_0CF_1-related, proton-conducting pathways are discriminated from others by their sensitivity to nucleotides (a and b) and/or inhibitors of CF_0, such as venturicidin, DCCD, or organotins (Linnett & Beechey, 1979).

Proton slip is elicited when thylakoids are suspended in alkaline media without nucleotides. This has been inferred from a diminished extent of proton uptake (McCarty et al., 1971; Evron & Avron, 1990) and an enhanced rate of linear electron flow (uncoupling of electron flow) under continuous illumination (Mukohata et al., 1975; Schönfeld & Neumann, 1977; Underwood & Gould, 1980; Evron & Avron, 1990). Proton slip has also been inferred from an accelerated decay of electrochromic absorption changes under flashing light (Gräber et al., 1981; Junge et al., 1992). Proton slip is blocked by adding concentrations of ADP (McCarty et al., 1971; Mukohata et al., 1975; Gräber et al., 1981; Evron & Avron, 1990; Junge et al., 1992) that are lower than those required for ATP synthesis. It has been discussed that proton slip, mainly the one observed under a strong proton motive force, may play a regulatory role (Strotmann et al., 1986) or a protective role as an overvoltage or over-ΔpH valve (Evron & Avron, 1990).

In view of the relatively large concentrations of nucleotides and phosphate in the stroma of chloroplasts (see Discussion), we questioned this interpretation and instead considered sequential binding of nucleotides causing transition first from an enzyme state with proton slip (no nucleotides) to a state with reduced proton conduction (about 1 μM ADP) and then to a state with ATP synthesis ($\gg$1 μM ADP). The first transition might represent the initiation of the postulated alternating or rotating site mechanism (Boyer, 1989) of ATP synthesis. Occupation of the first site would be necessary to connect proton flow to the coupling mechanism. Occupation of the second site would unlatch this mechanism for the release of ATP into the medium. From there on these two sites alternated in the catalytic cycle. A key question in the context of this alternating mechanism was whether or not the nucleotide binding site that was responsible for blocking proton slip belonged to the subset of catalytic sites. According to our experimental results, the answer was positive. This prompted us to elaborate on a mechanical machine which gives a unified description of proton slip, unisite, and multisite ATP synthesis and hydrolysis.

MATERIALS AND METHODS

We investigated the transition from the slipping over the closed to the coupled state of the enzyme as a function of the concentration of nucleotides and phosphate on the one hand and as a function of the proton motive force on the other. We used thylakoid membranes and applied flash spectrophotometry to monitor the decay of the flash-induced transmembrane voltage and pH transients on both sides of the membrane. This yielded not only the total specific conductance of the membrane but also the contribution of protons to this conductance (complete tracking of proton flow). As in

† This work was supported financially by the Deutsche Forschungsgemeinschaft (SFB 171/B3 and Graduiertenkolleg Zellbiologie/Osnabrück) and the Fonds der Chemischen Industrie.

‡ This article is dedicated to Britton Chance of Philadelphia at the occasion of his 80th birthday.

[1] Abbreviations: AdN, adenine nucleotides; CF_0, proton channel of the chloroplast ATPase; CF_1, peripheral, catalytic part of the chloroplast ATPase; Chl, chlorophyll; DCCD, *N,N'*-dicyclohexylcarbodiimide; HEPES, *N*-(2-hydroxyethyl)piperazine-*N'*-2-ethanesulfonic acid; PEP, phosphoenolpyruvate; PK, pyruvate kinase (EC 2.7.1.40); Tricine, *N*-[2-hydroxy-1,1-bis(hydroxymethyl)ethyl]glycine.

0006-2960/93/0432-8103$04.00/0

previous work on coupled proton flow by CF_0CF_1 (Junge, 1987) and uncoupled proton flow through CF_0 (Schönknecht et al., 1986; Althoff et al., 1989), the contributions of the ATPase were extracted from the total decay rate by their sensitivity to venturicidin.

Preparation of Thylakoids. Stacked thylakoids were prepared from 10–12-day-old pea seedlings as described (Polle & Junge, 1986). Concentrated stocks of thylakoids with 5 mM chlorophyll were stored on ice in a suspension medium of 10 mM Tricine (pH 7.8), 100 mM sorbitol, 10 mM NaCl, and 5 mM $MgCl_2$. Fresh stock lasted for at least 4 h without signs of aging.

Measurement of Flash-Induced Absorption Changes. Flash spectrophotometric measurements were carried out as described elsewhere (Junge, 1976). Thylakoids were suspended at an average chlorophyll concentration of 10 μM in a reaction medium containing 10 mM Tricine, 3 mM $MgCl_2$, and 10 μM methyl viologen, and the pH was adjusted to pH 8.0 using NaOH. Nucleotides and Na_2HPO_4 were added as indicated in the figure legends. For measurements of pH transients at the lumenal surface of the thylakoid membrane, Tricine was omitted and replaced by bovine serum albumin (2.6 mg/mL) as a selective (i.e., not membrane-permeable) buffer for the suspension medium (Ausländer & Junge, 1975). The thylakoid suspension was filled into an optical cell with a 2-cm optical path length and 15-mL volume. It was excited by short and saturating flashes of red light (>610 nm, 1 mJ/cm^2) and probed by a constant background of continuous measuring light (interference filter: 522 nm, intensity 200 μW/cm^2; or, for comparative measurements of pH transients and electrochromic transients (Figures 3 and 4), band filter: Schott DT-grün, 495–595 nm, intensity 1500 μW/cm^2). When thylakoid membranes are excited with short, single-turnover flashes of light, the photochemical reaction centers generate a voltage of 30–50 mV across the membrane, positive in the lumen, plus an acidification by less than 0.1 unit in the lumen (Junge, 1982). The transmembrane voltage was varied over a larger range by firing series of up to three light flashes at 2-ms intervals. Voltage and pH transients were generated at a repetition rate of 0.1 Hz. The transmembrane pH difference was varied by altering the intensity of the continuous measuring light. The electric potential difference across the thylakoid membrane, which was generated by flash groups, was measured by electrochromic absorption changes. pH transients in the suspending medium were detected using the pH-indicating dye, cresol red (Junge & Polle, 1986), and pH transients at the lumenal surface of the thylakoid membrane were detected by neutral red (Ausländer & Junge, 1975; Junge et al., 1979, 1986; Hong & Junge, 1983). Changes of absorption at 548 and 575 nm, obtained in the presence and the absence of the respective dyes, were subtracted in order to eliminate signal components caused by reactions other than pH transients. To improve the signal-to-noise ratio, 20 transient signals typically were averaged on a transient recorder (Tracor Northern TN 1500).

Biochemicals. ADP and ATP of high purity were purchased from Boehringer Mannheim. PK, PEP, and GDP were from Sigma. Additional chemicals of analytical grade were supplied by Merck (Darmstadt). The AdN contamination of GDP was checked by the luciferase assay. Luciferase is specific for ATP (Lee et al., 1970; McElroy & DeLuca, 1973). The ADP content was determined by conversion of ADP into ATP using a PEP/PK-coupled assay. The assay medium contained 50 mM HEPES, 100 mM KCl, 20 mM $MgSO_4$, 1 mM GDP, and 10 units/mL PK. The conversion was completed after

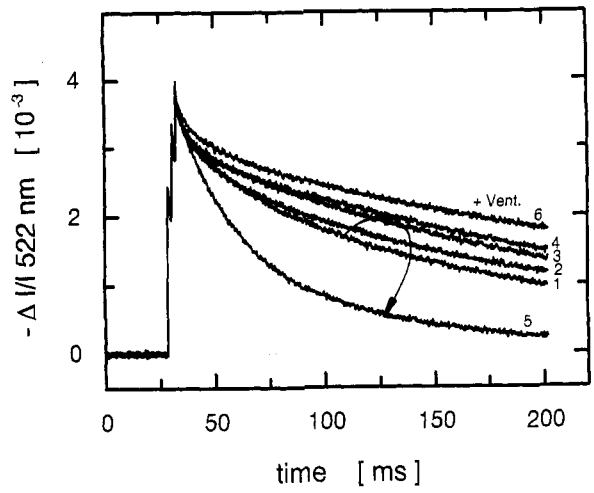

FIGURE 1: Effect of increased ADP concentration on electrochromic absorption changes in stacked thylakoid membranes. Transient electrochroism at 522 nm under excitation of thylakoids with flashing light. The reaction medium contained thylakoids equivalent to 10 μM Chl, 10 mM Tricine, 3 mM $MgCl_2$, 0.5 mM Na_2HPO_4, and 10 μM methyl viologen at pH 8.0. The curved arrow indicates increasing concentrations of ADP starting at 0 (1), 0.1 (2), 0.5 (3), 1 (4), and 100 μM (5). Curve 6 was obtained in the presence of 1 μM venturicidin. Decay curves as documented in this figure were the basis for the evaluation of rate constants plotted in the following figures. Note that rates were taken at the same voltage (not time) to account for nonohmic behavior.

20 min at room temperature. The AdN contamination of GDP was below 0.01%.

Analysis of Transient Electrochromic Signals. The magnitude of the proton current due to slip or coupled to ATP synthesis was determined at a given transmembrane voltage. The procedure for interpreting the decay of electrochromic absorption changes in terms of this current is sketched below and detailed further in the Appendix.

Electrochromic absorption changes as documented in Figure 1 were obtained in a thylakoid suspension with more than 10^{16} molecules of chlorophyll. The thylakoid system of one chloroplast contains more than 10^8 molecules of chlorophyll and 10^5 molecules of CF_0CF_1. It behaves as one coherent electric capacitor as shown by gramicidin titration (Schönknecht et al., 1990). Even if the voltage decay mediated by CF_0CF_1 was due to a small fraction of molecules, their number per vesicle was still large enough to assume that the same area-related specific conductance prevailed for any thylakoid. In other words, the suspension of more than 10^5 thylakoids was homogeneous as far as CF_0CF_1 was concerned.

Inspection of Figure 1, however, revealed a rapid initial decay phase of the electrochromic absorption changes even in the presence of venturicidin, which was added to block proton transfer through CF_0CF_1. The relative proportion of this initial decay was constant as a function of the initial extent of electrochromism which was varied through the energy of the light flash. Whether it was caused by a more leaky subset of (damaged) thylakoids or by a displacement current of limited magnitude is not yet clear. As it was apparently unaffected by nucleotides and inhibitors of the ATPase function, it was ignored. Only the absorption changes after completion of the rapid phase were analyzed. The electrochromic absorption changes from there on were taken as voltage transients.

In terms of the capacitor equation, the rate of voltage decay in a vesicle is proportional to the electric current density across the membrane. Here, the total current density at a given voltage was composed of contributions from CF_0CF_1 and from other sources. The contribution of the enzyme was calculated

as the difference of the current densities (at a given voltage) obtained in the absence and in the presence of a specific blocking agent (e.g., venturicidin). The current–voltage relationship of one enzymic channel may be nonohmic. This may be caused by the voltage dependence of the open probability of the channel and/or by nonohmic behavior of the open state. To eliminate the effect of the latter, the current densities were determined at a fixed voltage. Their variation as a function of the nucleotide concentration was interpreted in terms of a three-state model of the enzyme. Transitions from a slipping state over a closed one to a coupled state were brought forth by sequential binding of nucleotides at two binding sites according to Scheme I. Recordings of the ATPase-related current densities were plotted over the nucleotide or phosphate concentration and analyzed to yield the inhibition constant, K_i, and the Michaelis constant, K_m, as detailed in the Appendix.

Scheme I

$$E \xleftrightarrow{(K_i)} ADP,P_i{\cdot}E \xleftrightarrow{(K_m)} ADP,P_i{\cdot}E{\cdot}ADP,P_i$$

RESULTS

Nucleotide and Phosphate Dependence of Proton Slip. Figure 1 illustrates the sudden rise of the transmembrane voltage and its slower decay in thylakoids, which were excited with a group of three closely spaced flashes of red light. A short interval of 2 ms between consecutive flashes was chosen to increase the starting transmembrane voltage by the additive effect of about one turnover of photosystem I and three turnovers of photosystem II. The concentrations of Mg^{2+} and inorganic phosphate were 3 and 0.5 mM, respectively. The curved arrow follows the concentration of ADP, increasing from 0 to 100 μM. The slowest decay was observed when venturicidin was added. This curve was independent of the ADP concentration: it served as a control. Venturicidin blocks proton transfer through F-ATPases at the level of F_0 (Linnett & Beechey, 1979; Althoff et al., 1989; Galanis et al., 1989). An accelerated decay of the voltage, i.e., proton slip, was evident in the absence of ADP. The acceleration was diminished by 100 nM ADP and diminished further by increasing its concentration until the deceleration was counteracted and overcompensated by the acceleration, which was caused by proton translocation coupled to ATP synthesis. The accelerated decay of the transmembrane voltage by coupled transport of protons (Junge, 1970; Junge et al., 1970) and by slip (Gräber et al., 1981) has been described previously.

The relative decay rate of the transmembrane voltage (at a given voltage) as function of the concentration of ADP was corrected for the contribution of leak conductances, which were unrelated to CF_0CF_1 (see Materials and Methods), and plotted in Figure 2A. The curve represents a fit to the data according to the sequential reaction scheme (Scheme I) and eq 11 (see the Appendix). Each point is the average of the current densities obtained at three different voltages. The fit procedure gave the following parameters: K_i = 0.2 μM , the inhibition constant of the slip; K_m = 6.6 μM, the Michaelis constant of coupled proton flow. To clarify which type of nucleotide binding site (see Discussion) affects proton slip, we determined the effect of GDP on slip and coupled proton flow. The result is plotted in Figure 2B. GDP reduced slip, and at higher concentrations it stimulated coupled proton flow. The respective constants for GDP were K_i = 2.5 μM and K_m = 65 μM. It is noteworthy that the effect of GDP was not due to contamination with ADP (see Materials and Methods). ATP also reduced proton slip; K_i was 2 μM (not documented).

The inhibition of the slip by low concentrations of ADP and GDP required phosphate. Figure 2C shows the effect of phosphate at constant concentrations of ADP (1 μM) and Mg^{2+} (3 mM). It is evident that phosphate was required to diminish proton slip as it was required for coupled proton flow. The respective constants were K_i = 43 μM and K_m = 280 μM. We asked whether or not ADP inhibited slip without added phosphate. As is obvious from Figure 2D (in comparison to Figure 2A), ADP blocked proton slip even in the absence of phosphate, but the K_i value was larger by almost 2 orders of magnitude. This result favors a stochastic binding mechanism for ADP and P_i with the first substrate increasing the affinity for the second. The substitution of arsenate for phosphate (data not shown) produced the same conduction behavior, both for inhibition and synthesis, without significant changes in the K_i and K_m values for ADP. We also asked whether Mg^{2+}-ADP or just ADP was effective to block proton slip. When Mn^{2+} or Ca^{2+} was substituted for Mg^{2+} (3 mM), no inhibition of the slip by ADP was observed in the concentration range covered in Figure 2A.

Proton Specificity of Slip and Its Dependence on the Electrochemical Potential Difference of the Proton. In Figure 3 the transients of the transmembrane voltage and of the alkalinization of the suspending medium were compared. In the absence of nucleotides the decay of the transmembrane voltage was accelerated. The acceleration was diminished by the addition of ADP (1 μM) and more so by addition of venturicidin (1 μM) (Figure 3A). Figure 3B shows pH transients in the suspending medium. When venturicidin was added to block proton transfer through CF_0CF_1, the alkalinization due to proton uptake at both photosystems was apparent. The thylakoid membrane then became so proton-tight that the transmembrane pH difference lasted for more than 10 s (Junge et al., 1986). The rather slow rise of the alkalinization is attributable to the folded topology of stacked thylakoid membranes. It is due to lateral diffusion of protons through fixed buffering groups at the closely apposed membranes from the sites of rapid proton uptake (in less than 3 ms) toward the indicator molecules in the suspending bulk medium (Junge & Polle, 1986; Polle & Junge, 1986, 1989). In the absence of added nucleotides, the extent of the alkalinization was lessened. This was attributable to accelerated proton efflux from the thylakoid lumen as also evident from the accelerated charge flow in Figure 3A. Both proton efflux and charge flow were diminished by added ADP and venturicidin. This proved the proton specificity of slip under flashing light.

Figures 1 and 3 seemed to suggest that proton slip ended at a certain voltage. For coupled proton flow under ATP synthesis, a threshold voltage has been previously described (Junge, 1970; Junge et al., 1970). Under continuous light, or with artificially generated proton motive force, there is truly a threshold of the proton motive force with both its components, the electrical one ($\Delta\psi$) and the chemical one (ΔpH), equivalent to each other (Junesch & Gräber, 1985, 1991). We asked for the threshold of proton slip as a function of the flash-induced transmembrane voltage and the transmembrane pH difference. Since neither the transmembrane voltage nor the rather small pH differences have been calibrated so far with sufficient precision, the following considerations are merely semiquantitative. A group of three closely spaced flashes generates a voltage jump of about 100 mV (Junge, 1982) but a much smaller equivalent of chemical driving force (about 0.2 pH unit (Junge et al., 1979). By virtue of their different origins, the voltage (flash-induced)

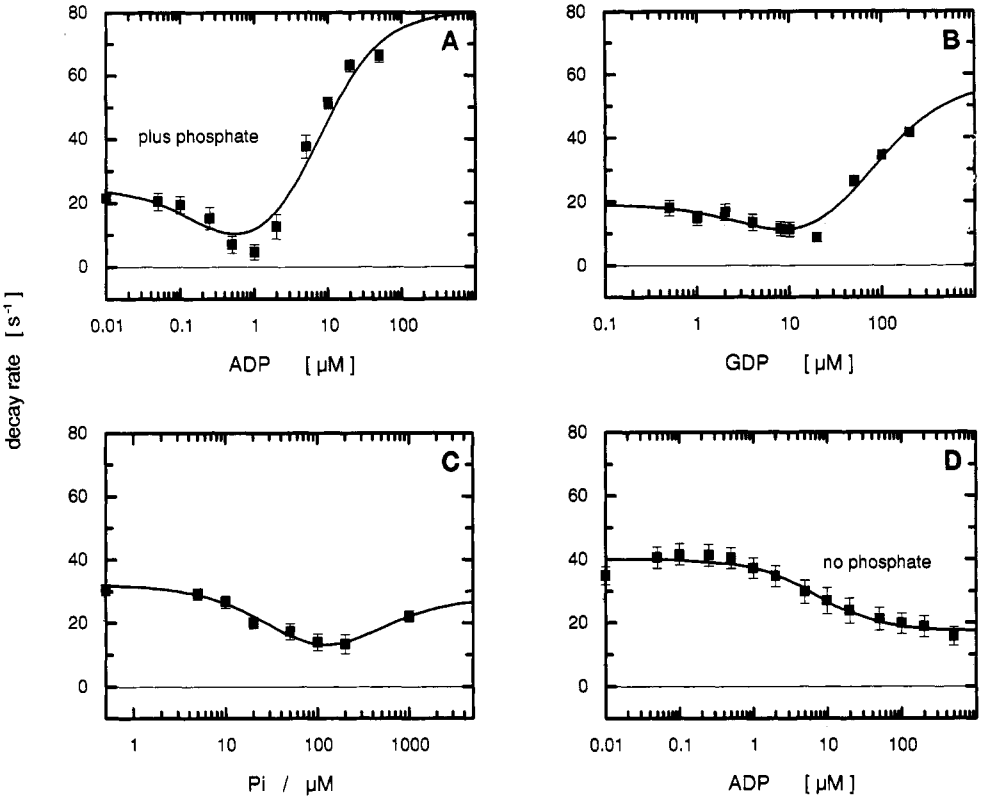

FIGURE 2: Decay rate of the flash-induced voltage as a function of ADP, GDP, and P_i. The relative decay rate (in s^{-1}) was calculated from data as documented in Figure 1 by the procedure described in the Appendix. The experiments presented in A and B were carried out in a reaction medium as described in Figure 1. In D phosphate was omitted. The phosphate dependence (C) was obtained in the presence of 1 μM ADP in the reaction medium. The symbols represent an average decay rate which was obtained from the decay rates at three different transmembrane voltages.

and the pH difference (continuous light induced) could be varied separately. We kept the flash-generated voltage transient constant and varied the underlying pH difference either by addition of an electroneutral uncoupler (Figure 4) or by the intensity of the continuous background light (Figure 5). In another approach the voltage was varied by the number of flashes, whereas the pH difference was kept constant (not shown).

Was proton slip still expressed if the background pH difference was eliminated? Figure 4 shows transients of the voltage, the pH in the lumen, and the pH in the suspending medium. They were obtained in the absence of added nucleotides. As is obvious from Figure 4A, the rapid decay of the voltage, which was characteristic for proton slip, was decelerated upon the addition of nigericin. That nigericin acted in the known way as an electroneutral proton/potassium exchanger was obvious from Figure 4B,C. The upper curves in Figure 4B,C are controls obtained in the presence of venturicidin but in the absence of nigericin. They revealed the transient acidification of the lumen (Figure 4A) and the transient alkalinization of the medium (Figure 4B). The transmembrane pH difference was rapidly equilibrated by the addition of nigericin (lower traces). The decay of the transmembrane voltage, on the other hand, was slowed down by nigericin (Figure 4A). Thus proton slip was inhibited if the voltage step was not backed up by a sufficiently large difference of the transmembrane pH. This was corroborated by the results represented in Figure 5. Here the background pH difference was varied by altering the intensity of the continuous measuring light. Figure 5 shows the CF_0CF_1-related decay rate of the transmembrane voltage as a function of the intensity of background illumination, which determined the background pH difference. As in the case of enzyme activation and ATP synthesis (Junesch & Gräber, 1987), an energetic threshold of proton slip could be inferred.

If the intensity of the continuous light, and thereby the pH difference, was kept constant (0.5 mW/cm²), and if the flash-induced voltage was varied by using 1, 2, or 3 flashes, proton slip was apparent after three flashes but not after only one flash. If the intensity of the continuous light was increased 2-fold (1 mW/cm²), on the other hand, proton slip was apparent even after a single flash (not documented).

Even at the present semiquantitative level, it was obvious that proton slip is only expressed above a threshold of the proton motive force. The electrical and the chemical components of this force seemed to be equivalent.

DISCUSSION

Proton Slip and Nucleotide Binding Sites. F-ATPases of chloroplasts, eubacteria, and mitochondria contain a total of six nucleotide binding sites (Engelbrecht & Junge, 1987; Girault et al., 1988; Shapiro et al., 1991). From a structural point of view these binding sites fall into two categories: three sites located at the interfaces between the α and β subunits, and three sites located exclusively on the β subunits (Kironde & Cross, 1987; Vogel & Cross, 1991). Considering that the 3-fold symmetry of the $(\alpha\beta)_3$ portion of the F_1 moiety (Tiedge & Schäfer, 1989) is broken by the smaller subunits (γ, δ and ε) (Gogol et al., 1990; Boekema & Böttcher, 1992), the three pairs of binding sites may divert into two or even three structurally different classes. An alternating site or rotatory catalytic mechanism, as has been proposed (Boyer, 1989), made the latter classification only transitory. The binding properties, namely, nucleotide specificity, affinity, and exchangeability, and the functions, namely, catalytic, noncatalytic, regulatory, and structural, are also complex.

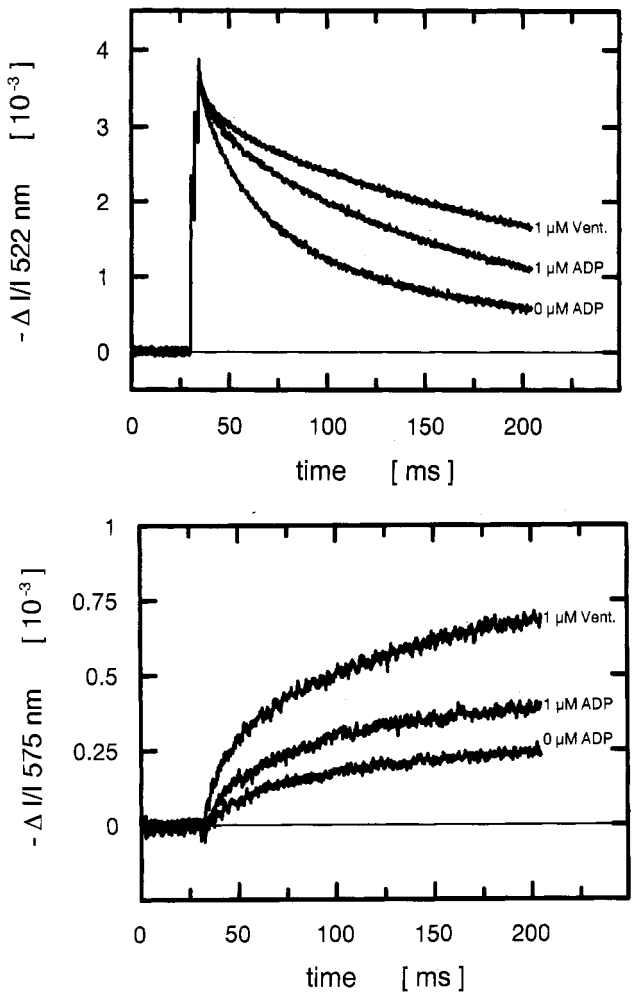

FIGURE 3: Effect of nucleotide binding on electrochromic absorption changes (A, top) and pH transients in the medium (B, bottom). (A) Transient electrochroism at 522 nm. (B) pH transients in the medium detected by cresol red. Increasing absorption indicates alkalinization of the suspending medium. ADP and venturicidin were added as indicated, and $[P_i] = 0.5$ mM. The intensity of the measuring light beam was 1500 $\mu W/cm^2$ (Schott DT-grün). The ordinate scale gives relative changes of transmitted intensity, $\Delta I/I$, at 522 and 575 nm, respectively.

It is not astounding that a comprehensive classification of the six sites is still lacking. Tight binding sites have been associated with a regulatory function, as the exposure of the membrane-bound enzyme to proton motive force leads to the release of tightly bound ADP with concomitant activation (Harris & Slater, 1975; Magnusson & McCarty, 1976; Strotmann et al., 1976; Huchzermeyer & Strotmann, 1977; Strotmann & Bickel-Sandkoetter, 1977). On the other hand, loose sites or readily exchanging sites have been named catalytic sites (Cross & Nalin, 1982; Cross et al., 1987; Guerrero & Boyer, 1988; Futai et al., 1989). Shapiro et al. have postulated one pair of noncatalytic and two pairs of catalytic sites (Shapiro et al., 1991). The properties within the catalytic pair may change during the operation of an alternating (or rotatory) mechanism. Following their argument, we adopted the following criterion for discrimination: The enzyme can synthesize/hydrolyze GTP as well as ATP at catalytic sites (Harris et al., 1978; Schlimme et al., 1979), whereas the tight binding sites only interact with adenine nucleotides (Wise & Senior, 1985; Kironde & Cross, 1986). We use the term, potentially catalytic sites, for those sites which can also bind guanidine nucleotides, independent of their affinity.

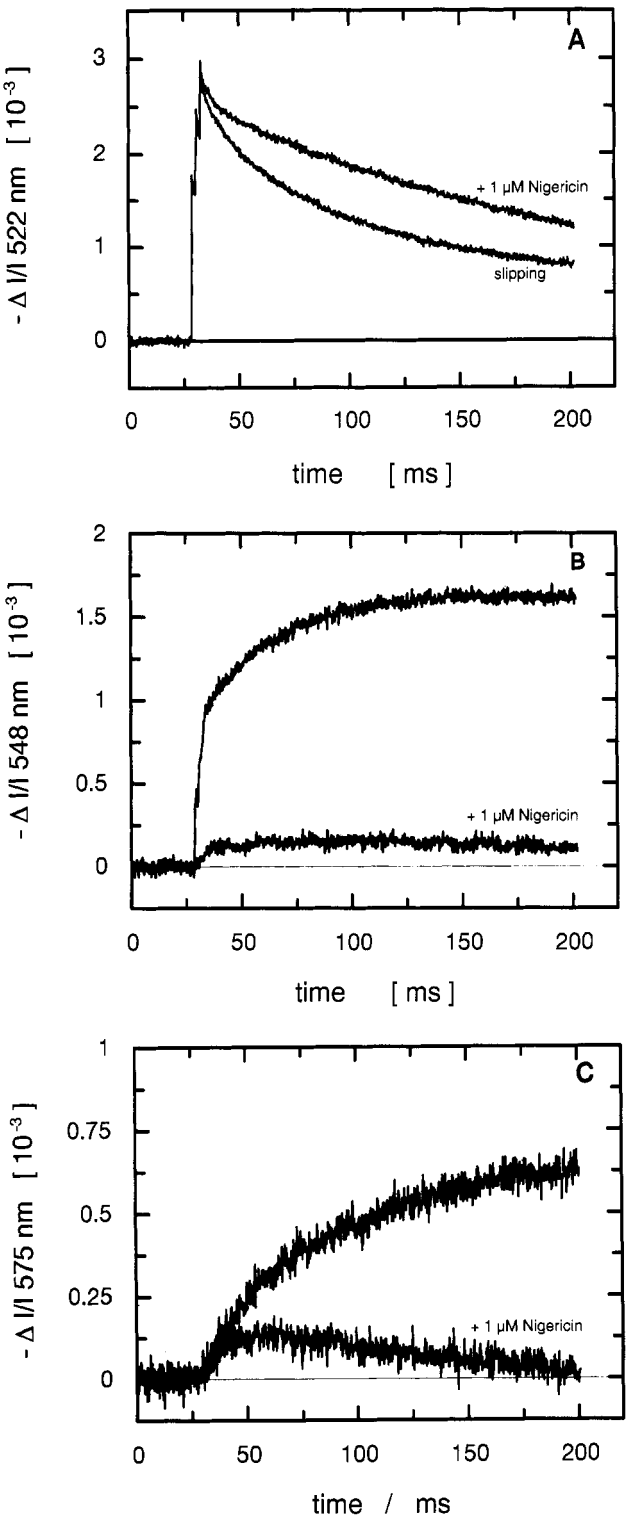

FIGURE 4: Effect of a steady pH difference on flash-induced proton slip. Transient electrochroism (A), pH transients in the lumen (B), and pH transients in the suspending medium (C). A was taken in the absence and in the presence of nigericin (1 μM). B and C were in the presence of nigericin (1 μM) and in its absence with venturicidin added (1 μM).

In most of the previous studies on proton slip, the nucleotide specificity was not addressed (Schönfeld & Neumann, 1977; Underwood & Gould, 1980; Gräber et al., 1981). In two reports an effect of GTP was tested and denied (McCarty et al., 1971; Evron & Avron, 1990). The binding sites responsible for the inhibition of proton slip were classified as regulatory ones (Evron & Avron, 1990). The concentration of GTP which was used in these studies, however, was the same as

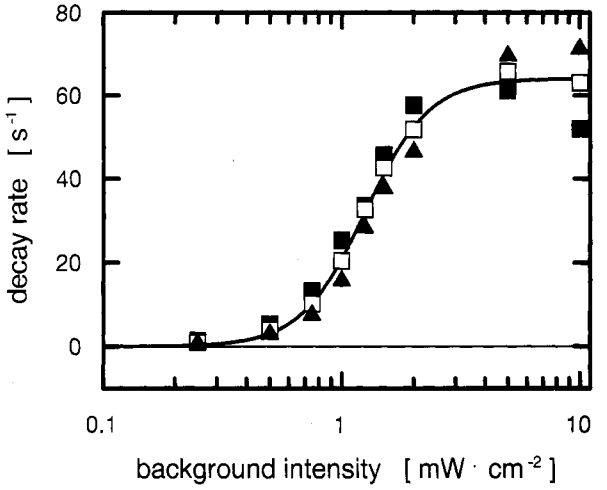

FIGURE 5: Threshold of proton slip. Relative decay rate (in s^{-1}) as a function of the intensity of continuous background light. The experiments were carried out in a reaction medium containing only the endogenous nucleotides of the ATPase (10 nM). The photosynthetic reactions were induced by a flash group consisting of three flashes plus a background illumination of varying intensity of measuring light (Schott DT-grün). The symbols correspond to decay rates taken at different transmembrane voltages. In terms of relative change of transmitted intensity at 522 nm the data sets were obtained at the following: (■) $\Delta I/I = -2.8 \times 10^{-3}$; (□) $\Delta I/I = -2.6 \times 10^{-3}$; (▲) $\Delta I/I = -2.4 \times 10^{-3}$.

that found for ATP in studies on the inhibition of proton slip. The affinity of the catalytic binding sites for guanine nucleotides, however, is known to be 10-fold lower than the one for ATP (Schlimme et al., 1979). Because of this, and in agreement with our data, the failure in the above-cited work to observe inhibition of proton slip by GTP may have been due to the low concentrations used.

There has been one report suggesting that phosphate is not required for the inhibition of proton slip by ADP [see Figure 2 in Gräber et al. (1981)]. To the contrary, the necessity of ADP plus phosphate plus Mg^{2+} has been demonstrated in another report (Evron & Avron, 1990); however, the K_i for phosphate was greater by 1 order of magnitude than in our work. Our studies showed that Mg^{2+}-ADP alone could inhibit proton slip; however, the affinity of the inhibitory binding site for Mg^{2+}-ADP was modulated by phosphate. Taken together, both the sensitivity to guanidine nucleotides and the greater effect of Mg^{2+}-XDP plus phosphate over Mg^{2+}-XDP alone led us to classify the nucleotide binding sites that are responsible for the inhibition of proton slip as potentially catalytic ones.

A regulatory function of proton slip has been proposed by Strotmann et al. (1986), and a function as safety valve against too large a proton motive force has been proposed by Evron and Avron (1990). Reports of the nucleotide concentration in the chloroplast stroma range from 0.64 to 1.8 mM for ATP and from 0.76 to 1.08 mM for ADP (Heineke et al., 1992). Phosphate was also found in the millimolar range (Sharkey & Vanderveer, 1989). These concentrations are much higher than the half-inhibitory concentrations that were observed in our work. This is difficult to reconcile with a regulatory or protective role for proton slip. This contradiction prompted us to search for an alternative reason for proton slip.

Proton Slip As a Consequence of the Alternating Site Mechanism of ATP Synthesis. We modeled a machine with a minimum set of elements to account for proton slip and coupled proton transport in terms of an alternating site mechanism of catalysis. It is illustrated in Figure 6. The elements of this machine are symbolic and not to be taken literally. That the proton carrier, as an example, is sketched as a rotating device with the rotation axis in the plane of the membrane serves illustrative purposes only. The carrier concept reaches further, of course (Stein & Läuger, 1990), and it can also incorporate the upward- and downward-directed motions that Fillingame postulated in his model of proton transport by F-ATPases (Fillingame, 1990).

The model machine consists of a proton carrier with two cooperative proton binding pockets and two cooperative nucleotide/phosphate binding sites. In addition to the cooperativity between the equivalent elements, there is crosswise interaction between the former and the latter elements. In Figure 6 the proton carrier is represented by a rotating device (large circle) embedded in the membrane (horizontal lines). It is equipped with two proton binding pockets, each of which may accommodate the three protons that are probably required for the synthesis of one molecule of ATP. The pockets interact in negative cooperativity. If one is flipped open, the other one is flopped into the closed conformation. Transitions between these two states are driven stochastically by thermal fluctuations. The rotor is surrounded by a stator imposing the following boundary conditions for rotational diffusion. Sliding along the stator elements is only feasible if one proton binding site is closed and the other one is protonated. Rotation is prohibited if the open binding pocket is empty. In the absence of additional elements (see below), the carrier is idling in stochastic rotatory diffusion. If there is no flip-flop between the binding pockets, the device just mediates proton exchange. With stochastic flip-flop, however, net proton transport occurs in the presence of a proton motive driving force. This describes the slipping state. It is illustrated in Figure 6, part 0.

A symmetrical lever represents two interacting nucleotide binding sites. It is attached to the rotor. As mentioned, we ignore all other nucleotide binding sites except two potentially catalytic ones. The intermediate-sized circles indicate ADP plus P_i and ATP, respectively. The first nucleotide binding site exposed is the one in close proximity to the open proton pocket (Figure 6, part 1). When a first set of substrate molecules binds tightly (i.e., with great loss of free energy) to the lever with an open binding pocket, the device is coupled. For further discussion of the mechanical model it may help to transpose the free energy of the ADP/P_i system into the mechanical potential of downward-directed gravity. In these terms the torque exerted by the bound nucleotide or the energy demand for lifting is too large to be readily overcome by thermal agitation. Rotational diffusion to support proton transport is practically prevented (but see further discussion). The proton carrier is now in its closed state (Figure 6, part 1).

The nucleotide binding sites cooperate such that the binding of the first set of substrate molecules to the left portion of the lever changes the affinity of the second site from very low (sketched at the tip of the right portion of the lever) to an intermediate level (closer to the center of the rotor). When the ADP concentration is sufficiently large, a second set of substrate molecules binds to this second site (Figure 6, part 2). This binding partially relieves the free energy constraints (in the mechanical analogon, the torque exerted by the "left" substrate is partially compensated by the "right" substrate). When the other constraint, i.e., the empty proton pocket, is also relieved by proton binding (Figure 6, part 3), thermally driven motion is reinstalled (Figure 6, part 4). Proton motive force, which is thought to be upwardly directed, favors proton intake from below and proton release above, which is equivalent to net clockwise rotational motion, again based on nondirec-

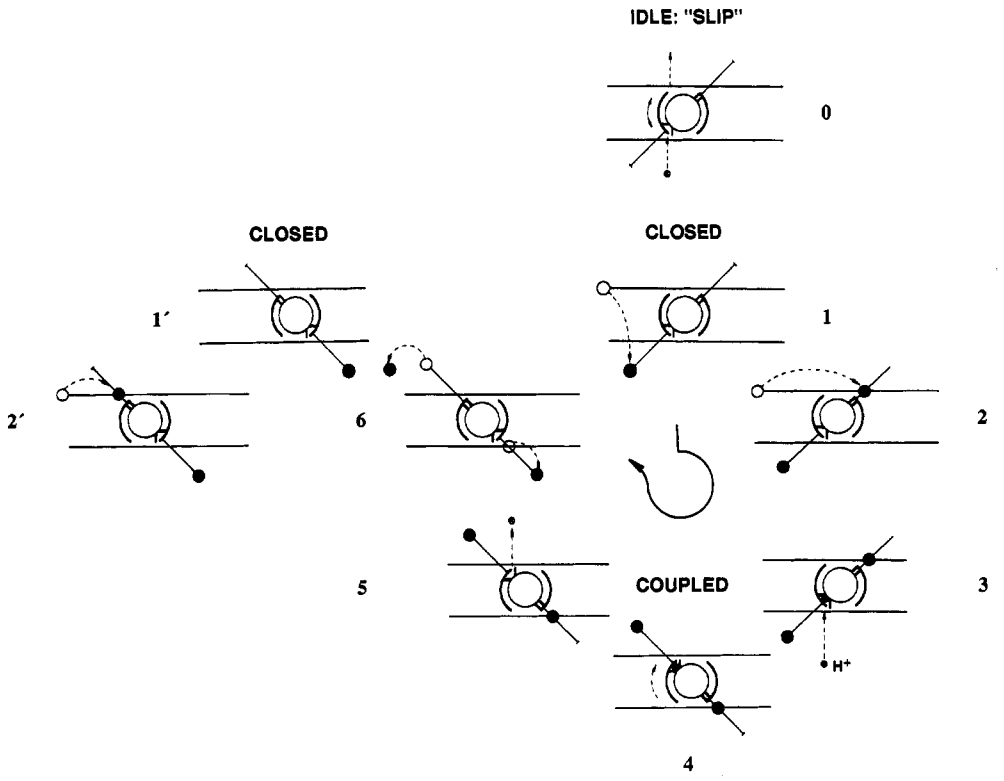

FIGURE 6: Model machine to visualize proton slip as a consequence of an alternating site mechanism of ATP catalysis. Terms taken from automotive technology to emphasize the mechanical character of the model.

tional rotational diffusion (Figure 6, parts 3–5). Thereby the first substrate pair, now as bound ATP, is lifted up to higher energy than before. Now follows a concerted set of three events (Figure 6, part 6): the release of proton(s), the release of bound ATP, and an energy drop of the second substrate from the low- into the high-affinity state of the binding site, which pulls the proximal proton binding pocket into its open state. The resulting configuration (Figure 6, part 1′) is the mirror image of the closed state depicted in Figure 6 (part 1), and it leads into the next, now counterclockwise, turn (Figure 6, parts 1′ and 2′), and so forth.

It is essential that the tight and loose binding sites change positions and that the ATP molecule produced originates from the ADP molecule which was bound in the step before last. It is also essential that the binding of ADP/P_i or of ATP to the end position of the lever pulls the proximal proton pocket into the open state and the distal one into the closed state. Under these conditions the reverse action, i.e., proton pumping at the expense of ATP hydrolysis, is self-explicatory.

The stochastic machine as sketched in Figure 6 not only gives a unified description of ATP synthesis/hydrolysis and proton slip but also gives a rationale for why the rates of unisite catalysis are smaller by several orders of magnitude than those for multisite catalysis (Grubmeyer et al., 1982; Fromme & Gräber, 1990a,b; Labahn & Gräber, 1990; Labahn et al., 1990). Unisite catalysis is viewed as the kinetically very much inhibited reaction which starts from the closed configuration of the enzyme (Figure 6, part 1). Even if protons are bound to the open pocket, the energy demand of lifting up the only bound ADP/P_i couple is too large to be readily overcome by thermal agitation. The reaction, though improbable, is still possible. Its completion to close the reaction cycle may involve the slipping state (Figure 6, part 0).

The binding characteristics of the tight site and the loose site as given in Figure 6 may be related to those of sites 1 and 3 in the nomenclature of Bruist and Hammes (1981) and Shapiro and McCarty (Shapiro & McCarty, 1988, 1990; Shapiro et al., 1991). Binding site 1 shows tight nucleotide binding, has a potentially catalytic function, and mediates exchange of ADP for ATP (see different K_i). Site 3 is characterized by the loose binding of adenine nucleotides and involvement in catalysis.

In conclusion, the nucleotide binding site which inhibits proton slip of the chloroplast ATPase binds ADP and phosphate or GDP and phosphate with high affinity. It is a potentially catalytic site. Because of its high affinity both for ADP and P_i as well as for ATP, and considering the large concentrations of these agents in the chloroplast stroma, a regulatory role or a protective role for slip is considered improbable if the affinities are not significantly lower under greater proton motive force. A model was presented consisting of a proton carrier with two proton binding pockets and two nucleotide binding sites. This stochastic model machine accounted for both coupled transport of protons with ATP synthesis and proton slip in the absence of nucleotides. It visualized slip as a consequence of an alternating site mechanism of ATP synthesis.

ACKNOWLEDGMENT

We thank our colleagues Holger Lill and Siegfried Engelbrecht for discussions and Hella Kenneweg for technical assistance.

APPENDIX

The decay of the transmembrane voltage is discussed in terms of the capacitor equation

$$i = c\frac{dU}{dt} \qquad (1)$$

where i denotes the current density in A/m^2, c the specific capacitance in F/m^2, U the voltage, and t the time. The current

density is related to the voltage by Ohm's law:

$$i = gU \tag{2}$$

where g is the specific conductance in S/m^2; to account for nonohmic behavior, it may be a function of the voltage.

$$g = g(U) \tag{3}$$

Three specific conductances are assumed to operate: $g_L(U)$, the leak conductance; $g_S(U)$, the proton conductance by CF_0CF_1 related to slip; $g_A(U)$, the proton conductance by CF_0CF_1 related to ATP synthesis. The leak conductance accounts for any conductor except CF_0 or CF_0CF_1. It remains if all CF_0 or CF_0CF_1 molecules are blocked by venturicidin or DCCD.

We assume that CF_0CF_1 can exist only in three states according to Scheme I involving two (nonequivalent) binding sites for ADP,P_i. In Scheme I, the bare enzyme, E, shows proton slip, the enzyme with one substrate, ADP,P_i·E, is closed, and the doubly loaded enzyme, ADP,P_i·E·ADP,P_i, couples proton flow to ATP synthesis. These states can be transformed into each other by sequential binding/release of ADP,P_i with two apparent dissociation constants: K_i (i for inhibition of slip) and K_m (m for midpoint of synthesis-coupled flow).

We assume that the association/dissociation of ADP,P_i has a much higher rate than any other reaction (e.g., ATP synthesis). Then the surface density of the enzyme state with proton slip, s (E), and that of the one which synthesizes ATP, a (i.e., ADP,P_i·E·ADP,P_i), are treated as equilibrium concentrations:

$$\frac{s}{e} = \left(1 + \frac{[\mathrm{AdN}]}{K_i} + \frac{[\mathrm{AdN}]^2}{K_iK_m}\right)^{-1} \tag{4}$$

$$\frac{a}{e} = \left(1 + \frac{K_m}{[\mathrm{AdN}]} + \frac{K_mK_i}{[\mathrm{AdN}]^2}\right)^{-1} \tag{5}$$

wherein e denotes the total surface density of CF_0CF_1 in m^{-2}.

The total current density is the sum of contributions from the three conductances named above:

$$i = (g_L + g_A + g_S)U \tag{6}$$

The specific conductance attributable to CF_0CF_1 molecules with the proton slip is

$$g_S = sG_S \tag{7}$$

and likewise

$$g_A = aG_A \tag{8}$$

The time-averaged single-enzyme conductances G_S and G_A are in Siemens, and they may be voltage-dependent, as stated.

The decay curves depicted in Figure 1 show a rapid phase even in the presence of venturicidin, seemingly indicative of a voltage dependence of the leak conductance, g_L. We found this not to hold; instead the fast drop was attributable to a fraction of particularly leaky vesicles or a displacement current of limited magnitude.

The nucleotide dependence of ATP synthesis and of proton slip was evaluated as follows. When the very rapid and venturicidin-insensitive decay was largely finished, but still at an extent of the electrochromic transient, where the slip was expressed, the slope of the voltage decay was determined, i.e.,

$$\left.\frac{dU}{dt}\right|_{U=U_y}$$

U_y denotes this given extent of the electrochromic absorption changes in terms of voltage. In the presence of venturicidin it yielded

$$\left.\frac{dU}{dt}\right|_{U_y}^{\mathrm{Vent}} = \frac{g_L(U_y)}{c}U_y \tag{9}$$

and in its absence,

$$\left.\frac{dU}{dt}\right|_{U_y}^{\mathrm{AdN}} = \frac{U_y}{c}[g_L(U_y) + g_A(U_y) + g_S(U_y)] \tag{10}$$

The CF_0CF_1-related conductance then was calculated according to

$$\frac{c}{U_y}\left(\left.\frac{dU}{dt}\right|_{U_y}^{\mathrm{AdN}} - \left.\frac{dU}{dt}\right|_{U_y}^{\mathrm{Vent}}\right) = \left(e\left(\left(1 + \frac{[\mathrm{AdN}]}{K_i} + \frac{[\mathrm{AdN}]^2}{K_iK_m}\right)^{-1}G_S + \left(1 + \frac{K_m}{[\mathrm{AdN}]} + \frac{K_mK_i}{[\mathrm{AdN}]^2}\right)^{-1}G_A\right)\right) \tag{11}$$

and fit using eq 11 to yield K_i and K_m. The fit procedures for P_i, GDP, and ATP were similar. Data were fit by a standard algorithm using the grafit software (Erithacus Software Limited, 1989).

REFERENCES

Althoff, G., Lill, H., & Junge, W. (1989) *J. Membr. Biol. 108*, 263–271.

Ausländer, W., & Junge, W. (1975) *FEBS Lett. 59*, 310–315.

Boekema, E. J., & Böttcher, B. (1992) *Biochim. Biophys. Acta 1098*, 131–143.

Boyer, P. D. (1989) *FASEB J. 3*, 2164–2178.

Bruist, M. F., & Hammes, G. G. (1981) *Biochemistry 20*, 6298–6305.

Cross, R. L., & Nalin, C. M. (1982) *J. Biol. Chem. 257*, 2874–2881.

Cross, R. L., Cunningham, D., Miller, C. G., Xue, Z., Zhou, J. M., & Boyer, P. D. (1987) *Proc. Natl. Acad. Sci. U.S.A. 84*, 5715–5719.

Engelbrecht, S., & Junge, W. (1987) *FEBS Lett. 219*, 321–325.

Evron, Y., & Avron, M. (1990) *Biochim. Biophys. Acta 1019*, 115–120.

Fillingame, R. H. (1990) in *Bacteria* (Krulwich, T. A., Ed.) Vol. 12, pp 345–391, Academic, San Diego, CA.

Fromme, P., & Gräber, P. (1990a) *Biochim. Biophys. Acta 1020*, 187–194.

Fromme, P., & Gräber, P. (1990b) *Biochim. Biophys. Acta 1016*, 29–42.

Futai, M., Noumi, T., & Maeda, M. (1989) *Annu. Rev. Biochem. 58*, 111–136.

Galanis, M., Mattoon, J. R., & Nagley, P. (1989) *FEBS Lett. 249*, 333–336.

Girault, G., Berger, G., Galmiche, J. M., & André, F. (1988) *J. Biol. Chem. 263*, 14690–14695.

Gogol, E. P., Johnston, E., Aggeler, R., & Capaldi, R. A. (1990) *Proc. Natl. Acad. Sci. U.S.A. 87*, 9585–9589.

Gräber, P., Burmeister, M., & Hortsch, M. (1981) *FEBS Lett. 136*, 25–31.

Grubmeyer, C., Cross, R. L., & Penefsky, H. S. (1982) *J. Biol. Chem. 25*, 12092–12100.

Guerrero, K. J., & Boyer, P. D. (1988) *Biochem. Biophys. Res. Commun. 154*, 854–860.

Harris, D. A., & Slater, E. C. (1975) *Biochim. Biophys. Acta 387*, 335–348.

Harris, D. A., Gomez-Fernandez, J. C., Klungsoeyr, L., & Radda, G. K. (1978) *Biochim. Biophys. Acta 504*, 364–383.

Heineke, D., Riens, B., Grosse, H., Hoferichter, P., Flügge, U.-I., & Heldt, H. W. (1992) *Plant Physiol. 95*, 1131–1137.

Hong, Y. Q., & Junge, W. (1983) *Biochim. Biophys. Acta 722*, 197–208.
Huchzermeyer, B., & Strotmann, H. (1977) *Z. Naturforsch., C: Biosci. 32C*, 803–809.
Junesch, U., & Gräber, P. (1985) *Biochim. Biophys. Acta 809*, 429–434.
Junesch, U., & Gräber, P. (1987) *Biochim. Biophys. Acta 893*, 275–288.
Junesch, U., & Gräber, P. (1991) *FEBS Lett. 294*, 275–278.
Junge, W. (1970) *Eur. J. Biochem. 14*, 582–592.
Junge, W. (1976) in *Chemistry and Biochemistry of Plant Pigments*, 2nd ed. (Goodwin, T. W., Ed.) Vol. 2, pp 233–333, Academic, London.
Junge, W. (1982) *Curr. Top. Membr. Transp. 16*, 431–465.
Junge, W. (1987) *Proc. Natl. Acad. Sci. U.S.A. 84*, 7084–7088.
Junge, W., & Polle, A. (1986) *Biochim. Biophys. Acta 848*, 265–273.
Junge, W., Rumberg, B., & Schroeder, H. (1970) *Eur. J. Biochem. 14*, 575–581.
Junge, W., Ausländer, W., McGeer, A., & Runge, T. (1979) *Biochim. Biophys. Acta 546*, 121–141.
Junge, W., Schönknecht, G., & Förster, V. (1986) *Biochim. Biophys. Acta 852*, 93–99.
Junge, W., Engelbrecht, S., Griwatz, C., & Groth, G. (1992) *J. Exp. Biol. 172*, 461–474.
Kironde, F. A. S., & Cross, R. L. (1986) *J. Biol. Chem. 261*, 12544–12549.
Kironde, F. A. S., & Cross, R. L. (1987) *J. Biol. Chem. 262*, 3488–3495.
Labahn, A., & Gräber, P. (1990) in *Current Research in Photosynthesis, Proceedings of the 8th International Conference on Photosynthesis, Stockholm, Sweden, August 6–11, 1989* (Baltscheffsky, M., Ed.) Vol. 3, pp 37–40, Kluwer, Dordrecht, The Netherlands.
Labahn, A., Fromme, P., & Gräber, P. (1990) *FEBS Lett. 271*, 116–118.
Lee, R. T., Denburg, J., & McElroy, W. D. (1970) *Arch. Biochem. Biophys. 141*, 38–52.
Linnett, P. E., & Beechey, R. B. (1979) *Methods Enzymol. 55*, 472–518.
Magnusson, R. P., & McCarty, R. E. (1976) *J. Biol. Chem. 251*, 7417–7422.
McCarty, R. E., Fuhrman, J. S., & Thuchiya, Y. (1971) *Proc. Natl. Acad. Sci. U.S.A. 68*, 2522–2526.
McElroy, W. D., & DeLuca, M. (1973) in *Chemiluminescence and Bioluminescence* (Cormier, M. J., Hercules, D. M., & Lee, J., Eds.) pp 285–311, Plenum, New York.
Mukohata, Y., Yagi, T., Sugiyama, Y., Matsunu, A., & Higashida, M. (1975) *Bioenergetics 7*, 91–102.
Polle, A., & Junge, W. (1986) *Biochim. Biophys. Acta 848*, 257–264.
Polle, A., & Junge, W. (1989) *Biophys. J. 56*, 27–31.
Schlimme, E., De Groot, E. J., Schott, E., Strotmann, H., & Edelmann, K. (1979) *FEBS Lett. 106*, 251–256.
Schönfeld, M., & Neumann, J. (1977) *FEBS Lett. 73*, 51–54.
Schönknecht, G., Junge, W., Lill, H., & Engelbrecht, S. (1986) *FEBS Lett. 203*, 289–294.
Schönknecht, G., Althoff, G., & Junge, W. (1990) *FEBS Lett. 277*, 65–68.
Shapiro, A. B., & McCarty, R. E. (1988) *J. Biol. Chem. 263*, 14160–14165.
Shapiro, A. B., & McCarty, R. E. (1990) *J. Biol. Chem. 265*, 4340–4347.
Shapiro, A. B., Huber, A. H., & McCarty, R. E. (1991) *J. Biol. Chem. 266 (7)*, 4194–4200.
Sharkey, T. D., & Vanderveer, P. J. (1989) *Plant Physiol. 91*, 679–684.
Stein, W. D., & Läuger, P. (1990) *Biophys. J. 57*, 255–267.
Strotmann, H., & Bickel-Sandkoetter, S. (1977) *Biochim. Biophys. Acta 460*, 126–135.
Strotmann, H., Bickel, S., & Huchzermeyer, B. (1976) *FEBS Lett. 61*, 194–198.
Strotmann, H., Kiefer, K., & Altvater-Mackensen, R. (1986) *Biochim. Biophys. Acta 850*, 90–96.
Tiedge, H., & Schäfer, G. (1989) *Biochim. Biophys. Acta 977*, 1–9.
Underwood, C., & Gould, J. M. (1980) *Arch. Biochem. Biophys. 204*, 241–246.
Vogel, P. D., & Cross, R. L. (1991) *J. Biol. Chem. 266 (10)*, 6101–6105.
Wise, J. G., & Senior, A. E. (1985) *Biochemistry 24*, 6949–6954.